



Ferroelectricity of $\text{Ca}_9\text{Fe}(\text{PO}_4)_7$ and $\text{Ca}_9\text{Mn}(\text{PO}_4)_7$ ceramics with polar whitlockite-type crystal structure

Umut ADEM

Department of Materials Science and Engineering, Izmir Institute of Technology, 35430, Urla, Izmir, TURKEY

Abstract

$\text{Ca}_9\text{Fe}(\text{PO}_4)_7$ is a member of the double phosphate family having polar whitlockite-type crystal structure. The phase transition from the room temperature polar $R3c$ to the high temperature non-polar $R\bar{3}c$ phase has been called a ferroelectric phase transition using complementary experiments such as temperature dependent second harmonic generation and dielectric constant measurements however no ferroelectric hysteresis measurement has been reported. In order to be able to call these polar materials ferroelectric, measurement of a saturated ferroelectric hysteresis loop is necessary to demonstrate that the electrical polarization of these materials is switchable. In order to realize this goal, we have synthesized $\text{Ca}_9\text{Fe}(\text{PO}_4)_7$ as well as structurally identical $\text{Ca}_9\text{Mn}(\text{PO}_4)_7$ using solid state synthesis. Crystal structure of the ceramics were confirmed using Rietveld refinement of the x-ray diffraction (XRD) patterns. Differential scanning calorimetry (DSC) measurements revealed phase transition temperatures of 848 and 860 K for $\text{Ca}_9\text{Fe}(\text{PO}_4)_7$ and $\text{Ca}_9\text{Mn}(\text{PO}_4)_7$, respectively. Our ferroelectric hysteresis measurements and current electric field loops (I-E) derived from the hysteresis loops showed that the loops cannot be saturated and the direction of the electrical polarization of both materials cannot be switched up to the largest applied electric field of 100 kV/cm. Possible origins of this behaviour are discussed.

Article info

History:

Received:20.04.2020

Accepted:31.05.2020

Keywords:

Ferroelectricity,
Phosphates, Rietveld
refinement,
Phase transitions.

1. Introduction

Calcium phosphate and vanadate compounds have been studied a lot as biomaterials [1-2] or for their luminescence properties [3-6]. Among them, double phosphates $\text{Ca}_9\text{R}^{3+}(\text{PO}_4)_7$ ($\text{R}^{3+}=\text{Al, Fe, Cr, Ga, Sc, In}$) are known to crystallize in polar whitlockite structure with $R3c$ space group [7-9]. There have been quite a few studies that focus on the ferroelectric nature of the phase transition between the polar low temperature and non-polar high temperature phases in both phosphates and vanadates [7-10]. Ferroelectric nature of this phase transition has been shown indirectly using x-ray diffraction, second harmonic generation, DSC, dielectric constant and electron diffraction experiments for example for $\text{Ca}_9\text{Fe}(\text{PO}_4)_7$ [8] among others. All these experiments on $\text{Ca}_9\text{Fe}(\text{PO}_4)_7$ point out to a phase transition from room temperature polar $R3c$ phase to a non-polar $R\bar{3}c$. However, strictly speaking, in order to be able to call these materials ferroelectric, switching of the electrical polarization of these samples must be demonstrated using ferroelectric hysteresis measurements. Otherwise, they can only be called

pyroelectric. In polar $\text{Ca}_9\text{Fe}(\text{PO}_4)_7$ structure, which is based on the whitlockite-type structure, there are six sites that Ca^{2+} and Fe^{3+} can occupy. M1-M3 sites are occupied by Ca^{2+} ions, Fe^{3+} occupies the M5 site of the whitlockite structure and M4 and M6 sites are unoccupied^{7,9}. A phase transition was reported to occur from polar $R3c$ phase to non-polar $R\bar{3}c$ phase at 890 K as shown by DSC measurements [8]. A peak in the dielectric constant was also reported around the same temperature. And the second harmonic generation signal disappears above the same temperature. All these experiments provide evidence to a polar-nonpolar phase transition. The phase transition into the non-polar phase was reported to involve disordering of the Ca^{2+} ions and orientational disordering of the PO_4 tetrahedra [8]. No literature on $\text{Ca}_9\text{Mn}(\text{PO}_4)_7$ could be found. As Mn^{3+} has a very similar ionic radius to other R^{3+} ions already studied in the family of $\text{Ca}_9\text{R}^{3+}(\text{PO}_4)_7$ ($\text{R}^{3+}=\text{Al, Fe, Cr, Ga, Sc, In}$), we have attempted to synthesize $\text{Ca}_9\text{Mn}(\text{PO}_4)_7$ and study its structural and ferroelectric properties as a comparison to $\text{Ca}_9\text{Fe}(\text{PO}_4)_7$.

In this manuscript, following the synthesis and structural characterization of the samples,

*Corresponding author. Email address: umutadem@iyte.edu.tr

ferroelectric hysteresis loops of $\text{Ca}_9\text{Fe}(\text{PO}_4)_7$ and $\text{Ca}_9\text{Mn}(\text{PO}_4)_7$ are reported for the first time in order to clarify whether the polarization is switchable in these polar materials with a high temperature polar-non polar phase transition.

2. Materials and Methods

$\text{Ca}_9\text{Fe}(\text{PO}_4)_7$ was synthesized using solid state synthesis following the method in [8]. Fe_2O_3 , CaCO_3 and $\text{Ca}_2\text{P}_2\text{O}_7$ powder were mixed using a mortar and a pestle in acetone medium and pressed into pellets of 13 mm diameter using a hydraulic press. The pellets were placed in alumina crucible and sintered at 1000°C for 6 hours in air. In order to obtain a pure phase, resulting pellets were crushed, ground, pelletized and sintered again under the same conditions. $\text{Ca}_9\text{Mn}(\text{PO}_4)_7$ was also synthesized using the same process from Mn_2O_3 , CaCO_3 and $\text{Ca}_2\text{P}_2\text{O}_7$ precursors. X-ray diffraction (XRD) patterns of the samples were collected using a Panalytical Empyrean diffractometer employing $\text{Cu K}\alpha$ source. Rietveld refinements of the collected XRD data were carried out using GSAS [11]. Differential Scanning Calorimetry (DSC) measurements were done using a Shimadzu DSC-60 Plus between room temperature and 600°C in the nitrogen atmosphere and using $5^\circ\text{C}/\text{min}$ heating rate. Ferroelectric hysteresis measurements were done at room temperature using an Aixacct TF Analyzer 1000. Dielectric properties were measured at room temperature using a Keysight E4980AL LCR Meter. For the electrical measurements, both surfaces of the pellets were coated with Ag epoxy and cured at 120°C for 20 minutes.

3. Results and Discussion

In Fig.1, refined XRD patterns of both $\text{Ca}_9\text{Fe}(\text{PO}_4)_7$ and $\text{Ca}_9\text{Mn}(\text{PO}_4)_7$ collected at room temperature are shown. For the refinements, crystallographic information files from the Materials Project [12] were used as the reference structure. All peaks belong to the whitlockite-type structure with the space group $R\bar{3}c$ and no impurity peaks could be detected. Good quality of the fits can be observed from the difference curve and low R_{wp} values for the samples: $R_{\text{wp}} = 5\%$ and 7.73% for $\text{Ca}_9\text{Fe}(\text{PO}_4)_7$ and $\text{Ca}_9\text{Mn}(\text{PO}_4)_7$, respectively. Refined lattice parameters are $a=10.3461(1)\text{ \AA}$, $c=37.191(1)\text{ \AA}$ and $a=10.3704(2)\text{ \AA}$, $c=37.2166(9)\text{ \AA}$ and for $\text{Ca}_9\text{Fe}(\text{PO}_4)_7$ and $\text{Ca}_9\text{Mn}(\text{PO}_4)_7$, respectively. Slightly larger lattice parameters of the $\text{Ca}_9\text{Mn}(\text{PO}_4)_7$ might be due to the presence of Mn^{2+} in the samples, in addition to the

expected Mn^{3+} . Mn^{2+} has a larger ionic radius [13] compared to Mn^{3+} and Fe^{3+} .

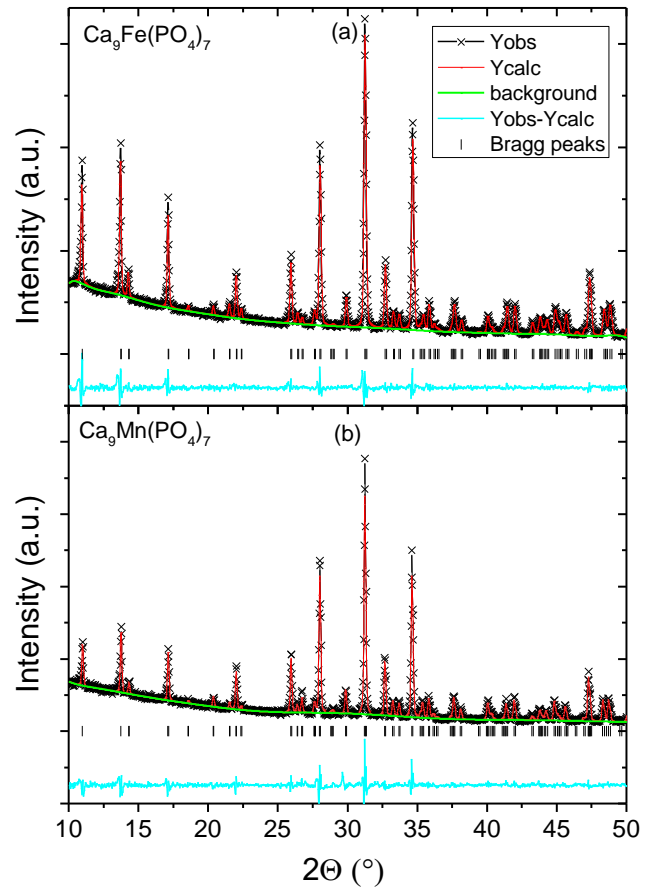


Figure 1. Refined x-ray diffraction patterns of (a) $\text{Ca}_9\text{Fe}(\text{PO}_4)_7$ and (b) $\text{Ca}_9\text{Mn}(\text{PO}_4)_7$. Black triangular symbols represent the collected data from the experiments, red solid lines show the calculated intensity, green lines show the background fits and light blue lines show the difference of experimentally observed and calculated intensities. Peak positions are marked with ticks.

In Figure 2, DSC curves of $\text{Ca}_9\text{Fe}(\text{PO}_4)_7$ and $\text{Ca}_9\text{Mn}(\text{PO}_4)_7$ are shown. In both materials, clear endothermic peaks are observed which correspond to the ferroelectric to paraelectric phase transition [9]. Estimated transition temperatures from DSC measurements are 848 and 860 K for $\text{Ca}_9\text{Fe}(\text{PO}_4)_7$ and $\text{Ca}_9\text{Mn}(\text{PO}_4)_7$, respectively. Transition temperature measured for $\text{Ca}_9\text{Fe}(\text{PO}_4)_7$ is slightly lower than the previously reported value (886 K) [8] whereas no previous studies could be found for $\text{Ca}_9\text{Mn}(\text{PO}_4)_7$. Dielectric constant and dielectric loss measured at RT and 1 kHz are tabulated in Table 1. Both samples have relatively low dielectric constant and loss, similar to the polar double phosphates with whitlockite-type structure reported in the literature [7-8]. Dielectric loss of $\text{Ca}_9\text{Mn}(\text{PO}_4)_7$ is slightly lower

than that of $\text{Ca}_9\text{Fe}(\text{PO}_4)_7$ which is reflected in the hysteresis loop measurements as we discuss below.

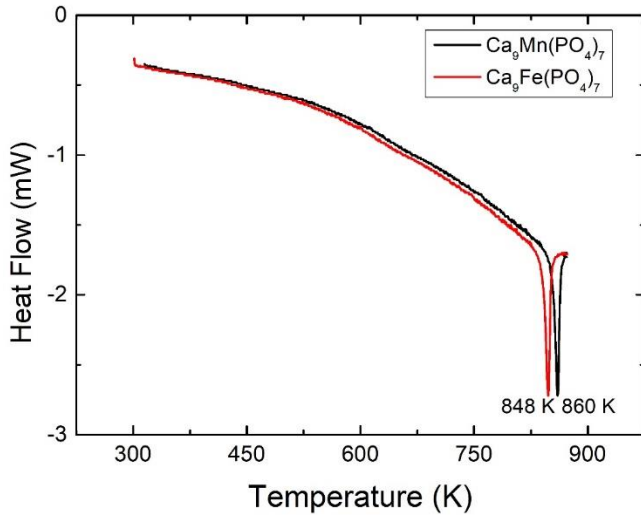


Figure 2. Temperature dependence of heat flow of $\text{Ca}_9\text{Fe}(\text{PO}_4)_7$ and $\text{Ca}_9\text{Mn}(\text{PO}_4)_7$.

Figure 3 shows the ferroelectric hysteresis loops of $\text{Ca}_9\text{Fe}(\text{PO}_4)_7$ as a function of applied voltage collected at 100 kHz. The loops show no saturation up to the largest applied electric field and preserve its linear behaviour with increasing voltage. Polarization value reaches around $0.5 \mu\text{C}/\text{cm}^2$ at the highest applied field of $\approx 85 \text{ kV}/\text{cm}$ which is smaller than the predicted value ($2\text{-}3 \mu\text{C}/\text{cm}^2$) based on the second harmonic generation experiments [8]. In the inset of Figure 3, frequency dependence of the hysteresis loop recorded at the highest applied voltage is shown. Significant frequency dependence could be observed: the loops transform from cigar-like shape at 1 Hz to almost linear shape at 100 kHz. Such relatively strong frequency dependence suggests conductivity contribution to the electrical polarization [14].

Table 1. Dielectric constant and dielectric loss values of $\text{Ca}_9\text{Fe}(\text{PO}_4)_7$ and $\text{Ca}_9\text{Mn}(\text{PO}_4)_7$ measured at room temperature and 1 kHz.

Material	Dielectric constant	Dielectric loss ($\tan\delta$)
$\text{Ca}_9\text{Fe}(\text{PO}_4)_7$	13	0.03
$\text{Ca}_9\text{Mn}(\text{PO}_4)_7$	7	0.023

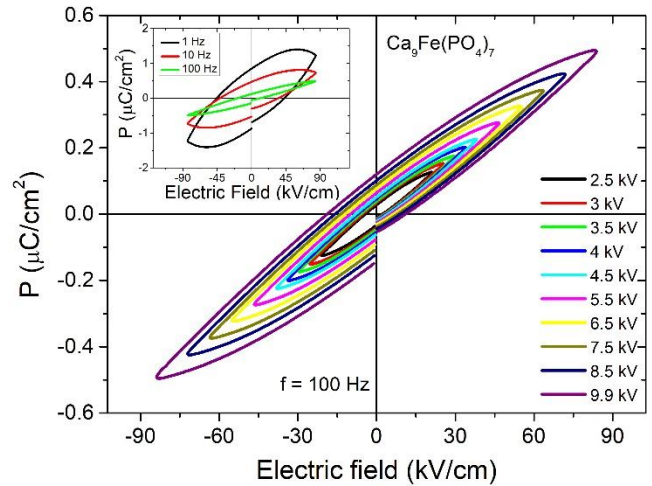


Figure 3. Ferroelectric hysteresis loops of $\text{Ca}_9\text{Fe}(\text{PO}_4)_7$ as a function of applied voltage at 100 Hz. Inset shows the frequency dependence of the polarization.

In Fig.4(a), hysteresis loops of $\text{Ca}_9\text{Mn}(\text{PO}_4)_7$ as a function of applied voltage are shown. Similar to $\text{Ca}_9\text{Fe}(\text{PO}_4)_7$, the loops measured at 10 kHz are not saturated and the polarization increases linearly with increasing voltage. In the inset of Fig.4(a), hysteresis loops measured at 1 and 10 Hz at the largest applied electric field are compared. Again similar to $\text{Ca}_9\text{Fe}(\text{PO}_4)_7$, electrical polarization is frequency dependent. Hysteresis loop has a cigar-like shape at 1 Hz, which changes to a slim linear behaviour at 10 Hz. Since the loops of $\text{Ca}_9\text{Fe}(\text{PO}_4)_7$ reach linear behaviour at lower frequencies compared to those of $\text{Ca}_9\text{Mn}(\text{PO}_4)_7$ (at 100 vs 10 Hz, respectively), we can conclude that the conductivity contribution to the electrical polarization is lower in $\text{Ca}_9\text{Mn}(\text{PO}_4)_7$ [14].

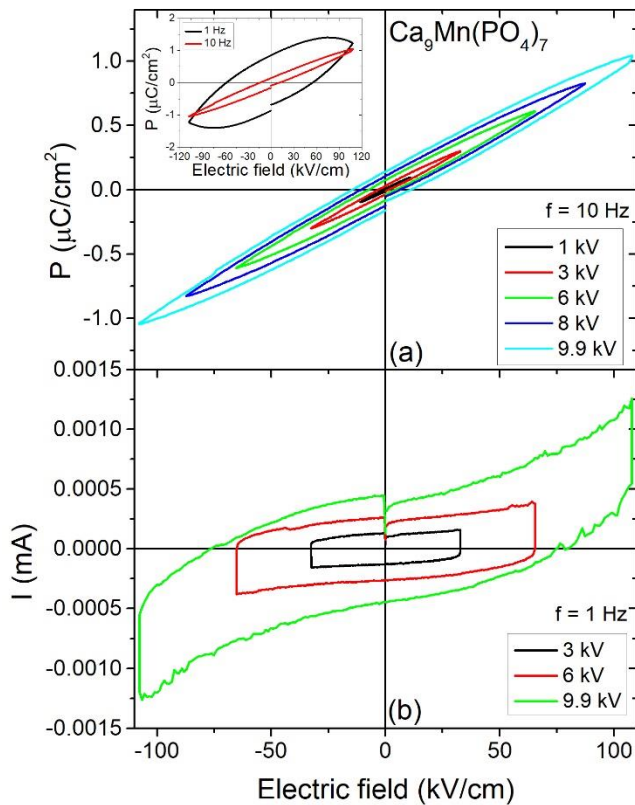


Figure 4. (a) Ferroelectric hysteresis loops of $\text{Ca}_9\text{Mn}(\text{PO}_4)_7$ as a function of applied voltage at 10 Hz. Inset shows the frequency dependence of the polarization compared at 1 and 10 kHz. (b) Current-electric field (I-E) curves of $\text{Ca}_9\text{Mn}(\text{PO}_4)_7$ at three different voltage values and 1 Hz.

In Fig.4(b), current-electric field (I-E) curves at three different voltage values are plotted. These curves can be extracted from hysteresis measurements and can be used together with the hysteresis loops, to assess switching of the electrical polarization and thus ferroelectricity. When the direction of the electric field changes, electrical polarization changes sign and this gives rise to a current peak for a ferroelectric. However, dielectric permittivity and electrical conductivity also contribute to the electrical current and may mask any peaks due to switching of the electrical polarization [15]. In our measurement, no current peaks can be observed in the curves obtained under 3 and 6 kV. In contrast, at 9.9 kV, which is the highest applied voltage, an emerging peak can be observed at the highest voltage. This emerging peak cannot be used as evidence for ferroelectricity as a proper peak is expected before the maximum electric field is reached for ferroelectric switching, but might still indicate that possible switching could be observed if larger electric field/voltage could have been applied [15].

Lack of ferroelectric switching is quite common in polar insulators. Two most common causes that prevent the observation of switching are (1) high activation energy for switching [16-18] and (2) large conductivity contribution masking the switching, due to the poor insulating nature of the material [15]. The former cause i.e. crystallographic switching path(s) for the ion(s) requiring a lot of energy typically leads to a very large coercive field and might cause dielectric breakdown to occur before the switching takes place. The latter cause is also quite common especially in multiferroic materials, most of which are poor electrical insulators [19-21]. In the case of calcium phosphates that we study here, both causes might be playing a role. Strong frequency dependence of the hysteresis loops points out that conductivity contribution is significant in these materials as we discussed above. Nevertheless, the emerging peak at the highest possible applied electric field/voltage for $\text{Ca}_9\text{Mn}(\text{PO}_4)_7$ might be a sign for possible switching at even larger electric fields, suggesting that the switching path is energetically costly. Further experiments on ceramics at higher fields or measurements on thin films (no thin films of double phosphates or vanadates have been reported so far) might be useful to clarify. In the literature of polar phosphates and vanadates, only one report showing hysteresis measurements can be found for $\text{Ca}_3(\text{VO}_4)_2$ [22], which is also isostructural to polar double phosphates and vanadates according to an early report [23]. Reported hysteresis loops are not saturated and hence no switching could be demonstrated. The lack of switching was attributed to the high coercive field of the material [22], similar to our case.

4. Conclusion

In conclusion, we attempted to clarify the ferroelectricity of polar double phosphates $\text{Ca}_9\text{Fe}(\text{PO}_4)_7$ and $\text{Ca}_9\text{Mn}(\text{PO}_4)_7$ with the whitlockite-type structure. Refined XRD patterns confirmed the crystal structure of the materials and DSC measurements yielded phase transition temperatures of 848 and 860 K for $\text{Ca}_9\text{Fe}(\text{PO}_4)_7$ and $\text{Ca}_9\text{Mn}(\text{PO}_4)_7$, respectively. Ferroelectric hysteresis measurements showed that the electrical polarization of both materials cannot be saturated up to the highest possible applied field and the polarization is also not switchable which can be evidenced from the lack of a peak in current-electric field (I-E) loops. Based on these results, strictly speaking, polar double phosphates $\text{Ca}_9\text{Fe}(\text{PO}_4)_7$ and $\text{Ca}_9\text{Mn}(\text{PO}_4)_7$ are pyroelectric rather than ferroelectric.

Acknowledgments

This work is supported by İzmir Institute of Technology (IZTECH) via BAP Project with the project number 2015İYTE29. We thank the IZTECH Department of Chemical Engineering for the DSC experiments and Celal Bayar University's DEFAM for the use of XRD.

Conflicts of interest

The author declares that he has no conflict of interests.

References

- [1] Dorozhkin S.V., Calcium orthophosphates in nature, biology and medicine, *Materials (Basel)*, 2 (2009) 399-498.
- [2] Engin N.Ö. and Taş A.C., Preparation of Porous $\text{Ca}_{10}(\text{PO}_4)_6(\text{OH})_2$ and $\beta\text{-Ca}_3(\text{PO}_4)_2$ Bioceramics, *J. Am. Ceram. Soc.*, 83 (2000) 1581-1584.
- [3] Zhu G., Li Z., Wang C. et al., Highly Eu^{3+} ions doped novel red emission solid solution phosphors, $\text{Ca}_{18}\text{Li}_3(\text{Bi},\text{Eu})(\text{PO}_4)_{14}$: Structure design, characteristic luminescence and abnormal thermal quenching behavior investigation, *Dalt. Trans.*, 48 (2019) 1624-1632.
- [4] Huang C.H., Chen T.M., Liu W.R., Chiu Y.C., Yeh Y.T. and Jang S.M., A single-phased emission-tunable phosphor $\text{Ca}_9\text{Y}(\text{PO}_4)_7:\text{Eu}^{2+},\text{Mn}^{2+}$ with efficient energy transfer for white-light-emitting diodes, *ACS Appl. Mater. Interfaces*, 2 (2010) 259-264.
- [5] Liang S., Dang P., Li G. et al. Controllable two-dimensional luminescence tuning in Eu^{2+} , Mn^{2+} doped $(\text{Ca},\text{Sr})_9\text{Sc}(\text{PO}_4)_7$ based on crystal field regulation and energy transfer, *J. Mater. Chem. C*, 6 (2018) 6714-6725.
- [6] Chen M., Xia Z., Molochev M.S., Wang T. and Liu Q., Tuning of Photoluminescence and Local Structures of Substituted Cations in $x\text{Sr}_2\text{Ca}(\text{PO}_4)_2-(1-x)\text{Ca}_{10}\text{Li}(\text{PO}_4)_7:\text{Eu}^{2+}$ Phosphors, *Chem. Mater.* 29 (2017) 1430-1438.
- [7] Morozov V.A., Belik A.A., Stefanovich S.Y. et al., High-temperature phase transition in the whitlockite-type phosphate $\text{Ca}_9\text{In}(\text{PO}_4)_7$, *J. Solid State Chem.*, 165 (2002) 278-288.
- [8] Lazoryak B.I., Morozov V.A., Belik A.A. et al., Ferroelectric phase transition in the whitlockite-type $\text{Ca}_9\text{Fe}(\text{PO}_4)_7$; crystal structure of the paraelectric phase at 923 K, *Solid State Sci.*, 6 (2004) 185-195.
- [9] Deineko D.V., Stefanovich S.Y., Mosunov A.V., Baryshnikova O.V. and Lazoryak B.I., Structure and properties of $\text{Ca}_{9-x}\text{Pb}_x\text{R}(\text{PO}_4)_7$ (R = Sc, Cr, Fe, Ga, In) whitlockite-like solid solutions, *Inorg. Mater.* 49 (2013) 507-512.
- [10] Belik A.A., Deyneko D.V., Baryshnikova O.V., Stefanovich S.Y. and Lazoryak B.I., $\text{Sr}_9\text{In}(\text{VO}_4)_7$ as a model ferroelectric in the structural family of $\beta\text{-Ca}_3(\text{PO}_4)_2$ -type phosphates and vanadates, *RSC Adv.*, 10 (2020) 10867-10872.
- [11] Larson A.C. and Von Dreele R.B., General Structure Analysis System (GSAS), *Los Alamos National Laboratory Report LAUR*, (2004) 86-748.
- [12] Jain A., Ong S.P., Hautier G. et al., Commentary: The Materials Project: A materials genome approach to accelerating materials innovation, *APL Mater.*, 1 (2013) 011002.
- [13] Shannon R.D., Revised effective ionic radii and systematic studies of interatomic distances in halides and chalcogenides, *Acta Crystallogr. Sect. A.*, 32 (1976) 751-767.
- [14] Jin L., Li F. and Zhang S.J., Decoding the Fingerprint of Ferroelectric Loops: Comprehension of the Material Properties and Structures, *J. Am. Ceram. Soc.*, 97 (2014) 1-27.
- [15] Yan H., Inam F., Viola G. et al., the Contribution of Electrical Conductivity, Dielectric Permittivity and Domain Switching in Ferroelectric Hysteresis Loops, *J. Adv. Dielectr.*, 01 (2011) 107-118.
- [16] Song S., Jang H.M., Lee N.S. et al., Ferroelectric polarization switching with a remarkably high activation energy in orthorhombic GaFeO_3 thin films, *NPG Asia Mater.*, 8 (2016) e242.
- [17] De C. and Sundaresan A., Nonswitchable polarization and magnetoelectric coupling in the high-pressure synthesized doubly ordered perovskites NaYMnWO_6 and NaHoCoWO_6 , *Phys. Rev. B.*, 97 (2018) 214418.
- [18] Garrity K.F., High-throughput first-principles search for new ferroelectrics, *Phys. Rev. B.*, 97 (2018) 024115.
- [19] Buurma A.J.C., Blake G.R., Palstra T.T.M. and Adem U., Multiferroic Materials: Physics and

Properties, *Reference Module in Materials Science and Materials Engineering*: <https://www.sciencedirect.com/science/article/pii/B9780128035818092456>, Elsevier Ltd., (2016).

- [20] Li M-R., Adem U., McMitchell S.R.C. et al., A polar corundum oxide displaying weak ferromagnetism at room temperature, *J. Am. Chem. Soc.*, 134 (2012) 3737-3747.
- [21] Catalan G. and Scott J.F., Physics and applications of bismuth ferrite, *Adv. Mater.*, 21 (2009) 2463-2485.
- [22] Ning H.P., Yan H.X. and Reece M.J., A High Curie Point Ferroelectric Ceramic $\text{Ca}_3(\text{VO}_4)_2$, *Ferroelectrics*, 487 (2015) 94-100.
- [23] Teterskii A.V., Morozov V.A., Stefanovich S.Y. and Lazoryak B.I., Dielectric and nonlinear optical properties of the $\text{Ca}_9\text{R}(\text{PO}_4)_4$ (R=Ln) phosphates, *Russ. J. Inorg. Chem.* 50 (2005) 986-989.